Kinetics of Zinc Oxide Reduction with Carbon Monoxide

C. E. GUGER AND F. S. MANNING

Reduction of ZnO single particles with CO was investigated at atmospheric pressure from 1000° to 1500°C. Weight loss data up to about 90 pct reduction were easily reproducible for the dense photoconductive grade ZnO particles but not for the American grade samples, whose scatter was attributed to the 13 pct residual internal porosity and to impurities. The data agreed closely with a mixed regime model, which pictures external diffusion acting in series with an irreversible first order kinetic process at the surface. After the diffusional contribution was subtracted, activation energies of 37,900 (±2040) cal per mole and 20,600 (±10,200) cal per mole were obtained for the photoconductive and American grades, respectively. For the photoconductive grade the mixed regime model gave a good fit over the entire temperature range. Diffusional limitations were approached at 1500°C.

ZINC extraction by thermal or electrothermal methods involves the overall reaction:

$$ZnO(s) + C(s) = Zn(g) + CO(g) \quad [1]$$

One mechanism for this process postulates a direct solid-solid reaction between the ZnO and the C,[1,2] while a second speculates a chain reaction involving the intermediate formation of CO and CO_2:[3-5]

$$ZnO(s) + CO(g) = Zn(g) + CO_2(g) \quad [2]$$

$$CO_2(g) + C(s) = 2CO(g) \quad [3]$$

The first mechanism appears to offer more resistance to the process because it restricts reaction to the points of contact between the ZnO and the C. Because of this, the second mechanism is accepted more readily, but neither of the stoichiometries is entirely satisfactory. The first cannot explain the formation of CO_2 in the furnace, while the second requires the initial presence of CO or CO_2 to initiate reduction. Reactions [2] and [3] may be initiated either by residual oxygen present in the furnace during start-up or else by oxygen generated by the thermal decomposition of ZnO:[6]

$$ZnO(s) = Zn(g) + \tfrac{1}{2}O_2(g) \quad [4]$$

The O_2 formed in this fashion could then react with the C to produce the CO required for reaction [2]:

$$C(s) + \tfrac{1}{2}O_2(g) = CO(g) \quad [5]$$

All of these reactions probably occur to some extent in a commercial zinc smelting shaft. The net contribution of each remains unknown at the present time.

This paper investigates reaction [2] both theoretically and experimentally, with particular emphasis being placed on isolating the chemical rate process at the surface from the physical rate processes of external mass transfer and internal diffusion. Previous studies employed porous samples with unusual geometries, which make it difficult to estimate the contribution of external and internal diffusion. The ultimate objective is to develop a process engineering model or design equation that would enable prediction and evaluation of multiparticle zinc smelting processes.

C. E. GUGER is Project Scientist, Koppers Co. Inc., Research Department, Monroeville, Pa. F. S. MANNING is Professor and Head, Department of Chemical Engineering, The University of Tulsa, Tulsa, Okla.

Manuscript received February 3, 1971.

LITERATURE REVIEW

Two types of mechanism have been proposed for the reduction of ZnO with CO. Type 1 mechanisms postulate the irreversible chemisorption of CO on the ZnO lattice with subsequent release of Zn and CO_2. The exact nature of the solid state surface phenomena has been discussed by Anderson,[7] Oates and Todd,[8] and more recently by Hauffe.[9] The other type of mechanism assumes the thermal decomposition of ZnO into Zn and O_2, which then diffuse into the bulk gas stream, where the O_2 reacts with any CO present.[10,11] In this case, the function of the CO is simply to establish the concentration gradients necessary for removing the Zn and O_2 from the surface, thus preventing their accumulation to equilibrium proportions.

Truesdale and Waring[12] measured rates of reduction from 800° to 1175°C by suspending a 1 in. diam by $\frac{1}{4}$ in. long ZnO disc into a $1\frac{1}{4}$ in. diam furnace tube from one arm of an analytical balance. Carbon monoxide was passed through the tube at a rate of 0.295 g per min per sq cm, and weight loss data obtained for the early stages of reduction. Fig. 1 illustrates the temperature dependence of Truesdale and Waring's initial reduction rates. From 800° to 1000°C Truesdale and Waring observed an apparent activation energy of 20 kcal per mole and concluded that reduction is controlled by surface reaction. The slight negative curvature seen at higher temperatures was attributed to an increasingly important contribution of a diffusion process, the nature of which was unspecified. Fig. 1, however, also shows predictions for a 1 cm diam spherical pellet and a CO velocity of 0.5 g per min per sq cm, computed by assuming that external diffusion controls at all temperatures. The external diffusion model[13] assumes that the surface reaction is sufficiently fast to guarantee a local equilibrium at the surface. For strongly endothermic reactions, such as ZnO reduction, the equilibrium constant increases rapidly with increase in temperature. When the reversibility of the reaction is considered, the hypothetical external dif-

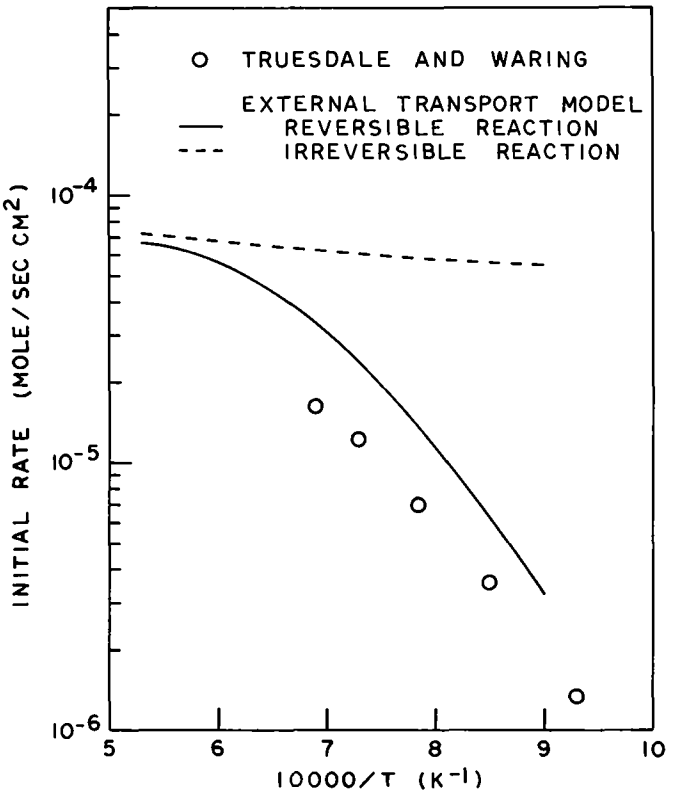

Fig. 1—Comparison of Truesdale and Waring's initial rate data with predictions of external transport model.

fusion model exhibits the same temperature dependence as Truesdale and Waring's data. Thus, a large apparent activation energy does not always imply a surface reaction limited process, nor does a change in activation energy always indicate a change in the rate-controlling step. Comparison of estimated diffusion rates with the observed overall rates is the only sure method of detecting kinetic control.

MIXED-REGIME REDUCTION MODEL

Reducing gases can attack both the external and internal surfaces of a ZnO pellet; the contribution of internal reduction, however, is small for dense pellets such as those used in the present study. External reduction involves:

1) Diffusion of CO through the external film or boundary layer surrounding the particle.

2) Reaction of the CO with the ZnO surface producing Zn vapor and CO_2.

3) Diffusion of the Zn and CO_2 through the boundary layer into the bulk gas.

It is noteworthy that for every mole of CO consumed at the surface, two moles of product gases are formed which stream away from the pellet. Thus, there is a net convection or bulk flow away from the particle, which makes it more difficult for the CO to approach the ZnO. If internal reaction is appreciable, three additional steps act in parallel with step 2 above:

4) Diffusion of CO into the interstices of the pellet.

5) Reaction of CO with the internal surface.

6) Counterdiffusion of the product Zn and CO_2 out of the pellet.

Since reduction is also endothermic, the external surface temperature of the ZnO specimen must drop so that heat can be received by:

7) Thermal radiation from the furnace walls.

8) Conduction, convection, and radiation from the surrounding gas.

If internal reduction is considerable, heat will also be transferred to the interior of the ZnO sample.

Development of a completely general model for the ZnO reduction process is prohibitively difficult for several reasons. First of all, pellet properties such as external diameter, external and internal surface areas, pore sizes, and so forth, change constantly, thus varying all transport and kinetic resistances. Secondly, estimation of diffusion fluxes (steps 1, 3, 4, and 6 above) is complicated because a three-component gas (CO, CO_2, Zn) is involved and because of the net convective flux away from the pellet. Finally, heat transfer effects are superimposed on this already complex mass transfer problem. In general, ZnO reduction is a multicomponent, nonequimolar, coupled reaction, mass, and heat transfer problem with moving external and internal boundaries. To obtain a first generation model, the following assumptions are made:

1) Internal reaction is negligible and the pellet is spherically symmetrical with no cracking or sintering.

2) A type 1 chemical mechanism is operating.

3) The system is isothermal; *i.e.*, heat fluxes do not have to be considered.

The first assumption is most critical because it determines the surface area exposed to the reducing atmosphere. It proves, however, to be adequate for dense pellets. A type 1 chemical mechanism is assumed because there seems to be more precedence for this type of mechanism. As for the third assumption, nonisothermal models can be developed for this system, but the multiparameter equations that result are extremely difficult to interpret and validate experimentally.

A mixed regime model requires that rate expressions be written for steps 1 to 3. Fortunately, preliminary estimates of multicomponent diffusion coefficients indicate that the diffusion coupling effect is roughly one-tenth the main diffusion effect for the CO-CO_2-Zn system. Diffusion coupling may therefore be neglected and all main diffusion coefficients treated as identical.[14] Steps 1 and 3, the flow of components through the boundary layer, may be written as the sum of diffusive and convective terms:

$$N_{CO} = -\mathfrak{D}C\frac{dy_{CO}}{dx} + (N_{CO} + N_{CO_2} + N_{Zn} + N_I)y_{CO} \quad [6]$$

$$N_{CO_2} = -\mathfrak{D}C\frac{dy_{CO_2}}{dx} + (N_{CO} + N_{CO_2} + N_{Zn} + N_I)y_{CO_2} \quad [7]$$

$$N_{Zn} = -\mathfrak{D}C\frac{dy_{Zn}}{dx} + (N_{CO} + N_{CO_2} + N_{Zn} + N_I)y_{Zn} \quad [8]$$

$$N_I = -\mathfrak{D}C\frac{dy_I}{dx} + (N_{CO} + N_{CO_2} + N_{Zn} + N_I)y_I \quad [9]$$

From the reaction stoichiometry (Eq. [2]),

$$R = -N_{CO} = N_{CO_2} = N_{Zn} \text{ and } N_I = 0 \quad [10]$$

Substituting Eq. [10] into [6] to [9] and integrating from

$x = 0$ where $y = y_b$ (bulk phase composition) to $x = \delta$ yields the gas composition at the surface:

$$y_{CO,s} = (1 + y_{CO,b}) e^{R\delta/C\mathfrak{D}} - 1 \quad [11]$$

$$y_{CO_2,s} = 1 - (1 - y_{CO_2,b}) e^{R\delta/C\mathfrak{D}} \quad [12]$$

$$y_{Zn,s} = 1 - (1 - y_{Zn,b}) e^{R\delta/C\mathfrak{D}} \quad [13]$$

$$y_{I,s} = y_{I,b} e^{R\delta/C\mathfrak{D}} \quad [14]$$

By direct analogy with the classic film model,[15] $\mathfrak{D}/\delta$ may be replaced by the mass transfer coefficient k, where k in turn, may be correlated [16] by

$$\frac{kD}{\mathfrak{D}} = 2.0 + 0.60 \left(\frac{DV\rho_g}{\mu}\right)^{1/2} \left(\frac{\mu}{\rho_g \mathfrak{D}}\right)^{1/3} \quad [15]$$

Eq. [15] shows that k varies with the particle diameter according to

$$k = \frac{\alpha}{D} + \frac{\beta}{D^{1/2}} \quad [16]$$

where α and β are dimensional constants.

Step 2, the surface reaction, may be modeled by a reversible reaction as suggested by the stoichiometry:

$$R = \frac{1}{SM}\frac{dw}{dt} = \frac{\rho}{2M}\frac{dD}{dt} = -k_r \left(C_{CO,s} - \frac{C_{CO_2,s} C_{Zn,s}}{K_c}\right)$$

$$= -k_r C \left[y_{CO,s} - \frac{y_{CO_2,s}\, y_{Zn,s}}{K/P}\right] \quad [17]$$

Eqs. [11], [12], [13], and [17] may now be combined to yield

$$R = k_r C \left\{\frac{P}{K}\left[1 - (1 - y_{CO_2,b}) e^{R/Ck}\right] \times \left[1 - (1 - y_{Zn,b}) e^{R/Ck}\right] - \left[(1 + y_{CO,b}) e^{R/Ck} - 1\right]\right\} \quad [18]$$

which is an implicit equation for the instantaneous rate of reduction, R. All quantities in this equation are constant except R and k, which vary as the particle diameter decreases. Eq. [18] is compatible with thermodynamics because it yields a zero rate of reduction when the bulk gas is at equilibrium. Unfortunately, the reduction rate cannot be solved explicitly, and numerical integration is required to determine the particle diameter as a function of time.

SIMPLIFIED MIXED-REGIME MODEL

Two simplifications can be introduced which permit not only explicit solution for the reduction rate but also analytical integration as well:

1) If the reduction rate, R, is small relative to Ck, the exponentials in Eq. [18] can be linearized to

$$e^{R/Ck} = 1 + \frac{R}{Ck} \quad [19]$$

This linearization introduces a maximum error of 28 pct in the reduction rate under the most extreme conditions, *i.e.*, pure CO at very high temperatures.

2) If the reaction is assumed to be essentially irreversible,

$$P y_{CO_2,s}\, y_{Zn,s} / K \ll y_{CO,s} \quad [20]$$

While this approximation is certainly questionable at low temperatures where K is small, the surface reaction becomes increasingly influential at low temperatures, and surface concentrations approach bulk phase values. Thus, for small concentrations of CO_2 and/or Zn in the bulk phase, this assumption is surprisingly useful.

These simplifications reduce Eq. [18] to

$$R = -\frac{C y_{CO,b}}{\frac{1}{k_r} + \frac{1}{k} + \frac{y_{CO,b}}{k}} \quad [21]$$

The terms, $1/k_r$, $1/k$, and $y_{CO,b}/k$ represent the resistances due to surface reaction, diffusion, and net convection, respectively. As expected, these resistances act in series. Substituting Eqs. [16] and [17] into [21] yields

$$\frac{\rho}{2M}\frac{dD}{dt}\left[\frac{1}{k_r} + \frac{(1 + y_{CO,b})}{\alpha/D + \beta/D^{1/2}}\right] = -C y_{CO,b} \quad [22]$$

Integrating between $t = 0, D = D_0$ and $t = t, D = D$ gives

$$t = \rho \frac{(1 + y_{CO,b}) D_0^2}{\alpha M C y_{CO,b}} \left\{\frac{(\psi - \gamma^2)}{2}\left[1 - \frac{D}{D_0}\right] + \frac{\gamma}{3}\left[1 - \left(\frac{D}{D_0}\right)^{3/2}\right] + \gamma^3\left[1 - \left(\frac{D}{D_0}\right)^{1/2}\right] + \gamma^4 \ln\left[\frac{\gamma + (D/D_0)^{1/2}}{1 + \gamma}\right]\right\} \quad [23]$$

where $\gamma = \alpha/\beta D_0^{1/2}$ and $\psi = \alpha/(1 + y_{CO,b}) D_0 k_r$. Eq. [23] provides the desired relationship between particle diameter and time for bulk gas compositions far removed from equilibrium.

EXPERIMENTAL APPARATUS AND PROCEDURE

Two grades of ZnO, supplied by the St. Joe Minerals Company, Monaca, Pennsylvania, were used in the experimental program—a pigment grade American process oxide and a high purity photoconductive grade oxide. Table I lists the reported impurities. Spherical pellets were pressed at room temperature using special stainless steel dies developed by N. C. Scrivner,[17] a coworker who was conducting a similar investigation into the kinetics of wüstite reduction. Mr. Scrivner's original dies were coated with Teflon to facilitate mold release, but this coating alone proved inadequate for pressing ZnO pellets. Reliable mold release was achieved by cleaning the die surfaces with hexane after every press. As long as the hexane was used regularly, no binder or excess moisture was needed. The pressed pellets were dried overnight at 150°F and then sintered in air in a Globar resistance furnace to reduce the porosity. Essentially zero pct porosity was achieved

Table I. Analysis of Zinc Oxide Samples

Impurity	American	Photoconductive
Fe_2O_3	0.0142 pct	0.001 pct
SiO_2	0.123 pct	0.002 pct
CdO	0.0033 pct	0.000177 pct
PbO	0.0095 pct	0.00102 pct
CuO	0.00070 pct	0.0001 pct
MnO	0.00163 pct	0.0005 pct
In_2O_3	0.00110 pct	0.00017 pct
Al_2O_3	0.053 pct	0.01 pct

for the photoconductive grade ZnO by sintering at 1000°C for 1 hr, whereas only 13 pct voidage was obtained for the American grade specimens by sintering at 1400°C for 2 hr. Porosities were calculated from pellet volumes determined by displacing tetrachloroethane in a 250 ml volumetric flask and measuring the displacement with a 1 ml pipette graduated to within 0.01 ml.

A thermogravimetric method was used to follow the kinetics of reduction. The pellets were suspended from a Ni Span C spring balance into an alumina reaction tube heated by a molybdenum-wound resistance furnace. The sensitivity of the spring was 0.602 cm per g, and spring displacements were followed with a cathetometer capable of reading to within 0.005 cm. The overall sensitivity of the balance system was therefore 8.3 mg, which was adequate because of the large weight loss accompanying ZnO reduction. The spring balance and upper suspension were protected from the hot furnace gases by means of a N_2 gas seal. The alumina seal tube was sufficiently long to prevent the reversible deposition of ZnO on the upper suspension. No ZnO deposited below the seal tube because of the higher temperatures there. The sample was located about 15 in. below the seal tube, and the downward seal gas flow was always small compared to the upward reducing gas flow.

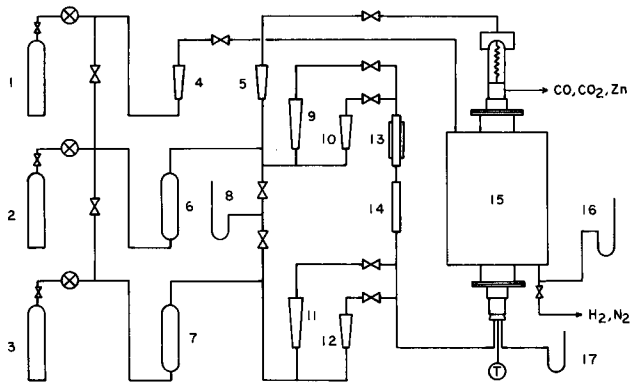

Fig. 2—Flow diagram of gas distribution system: 1, 2, 3—8 pct H_2-N_2 mixture, N_2 and CO gas cylinders, respectively; 4, 5, 9, 10, 11, 12—rotameters; 6, 7—magnesium perchlorate drying towers; 8—mercury manometer; 13—oxygen removal furnace; 14—copper base catalyst chamber for oxygen removal; 15—Lindberg Hevi Duty high temperature molybdenum-wound resistance furnace; 16, 17—water manometers.

The reactor consisted of a 2 in. ID by 60 in. long impervious alumina tube whose lower section was packed with alumina pellets to preheat the reducing gas. The hot junction of 30 gage Pt vs Pt 10 pct Rh thermocouple, inserted from the bottom through a $\frac{1}{4}$ in. alumina protection tube, was located $\frac{1}{2}$ in. below the sample. The cold junction was immersed in an ice bath, and the electromotive force measured to within 0.01 mv (0.83°C) with a portable potentiometer. The reduction tube was heated with a 4 in. diam molybdenum resistance furnace, having an overall length of 52 in. and a heated length of 24 in. Temperatures were controlled to within ±2°C with a Barber Colman proportional temperature controller. Fig. 2 shows the gas distribution system, which permitted feeding of CO or CO-N_2 mixtures to the reduction tube and N_2-H_2 mixtures into the furnace insulation compartment to prevent oxidation of the molybdenum resistance windings.

The experimental procedure was relatively straightforward. The pellet was weighed, placed in a Pt-10 pct Rh wire basket, suspended from the spring balance, and gently lowered into the reduction tube. A small hoist attached to the spring balance enclosure was used for inserting and removing the pellets from the furnace. While the pellet was being heated to reaction temperature, the reduction tube was purged with N_2. CO was then introduced and the spring position recorded at half-minute intervals above 1400°C and every minute below 1400°C. Temperature, pressure, and CO flow were measured periodically during the run.

RESULTS AND DISCUSSION

The scope of the experiments is presented in Table II. Many runs were terminated early to provide photo-

Table II. Scope of Experimental Data

Type of Oxide	American	Photoconductive
Initial pellet size, cm	0.77 to 1.4	0.98 to 1.0
Initial pellet weight, g	1.17 to 6.79	2.73 to 3.06
Reduction temperature, °C	1000 to 1400	1000 to 1500
CO Flow, g per sq cm per min	0.25 to 0.59	0.11 to 1.5
Reduction time, min	6 to 70	2 to 74
Final pct reduction	30 to 99	10 to 99

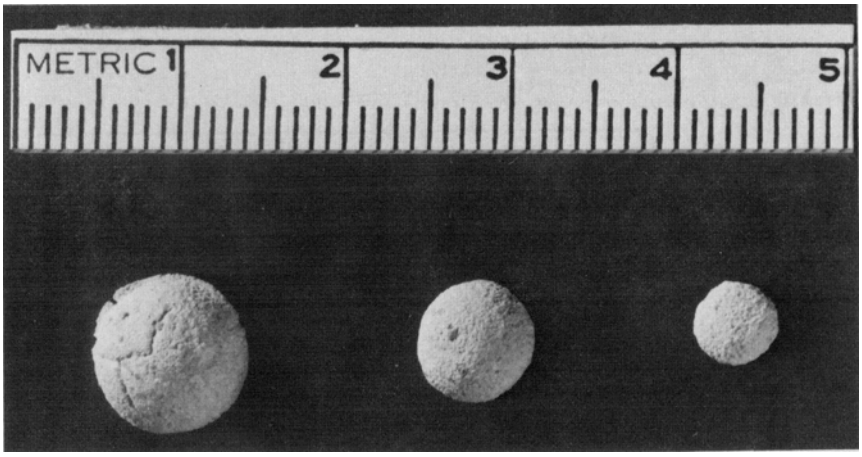

Fig. 3—Reduction of American grade ZnO pellets at 1000°C: 15, 38, and 58 min.

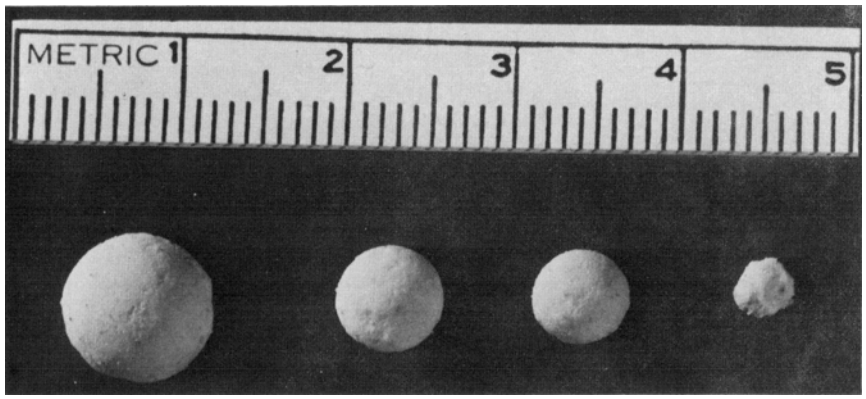

Fig. 4—Reduction of photoconductive ZnO pellets at 1400°C: 2, 5, 6, and 8 min.

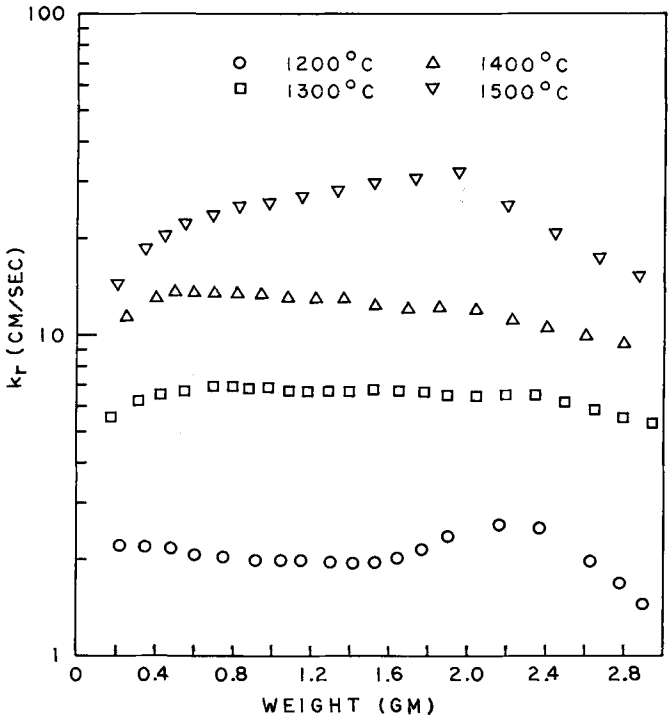

Fig. 5—Variation of first order rate constant during reduction of photoconductive grade ZnO samples.

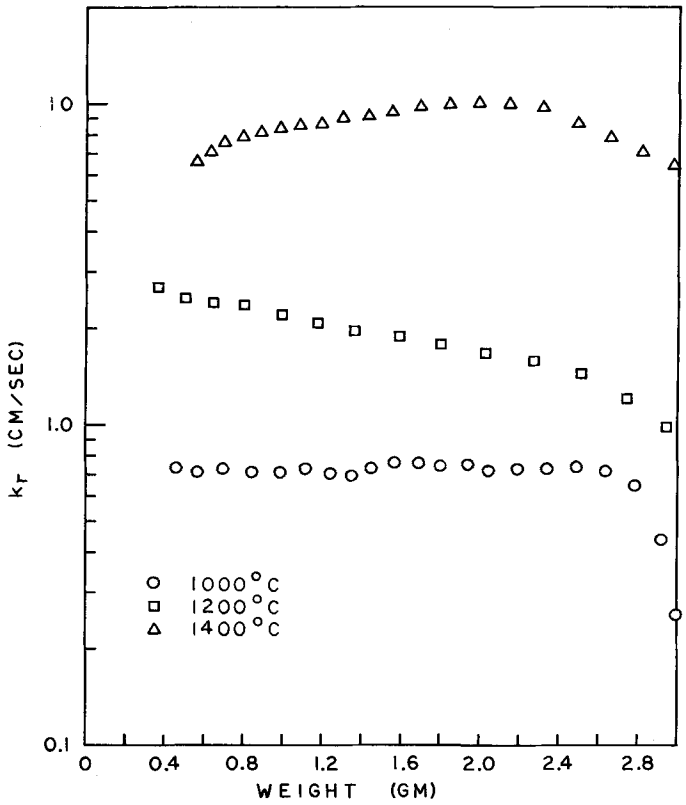

Fig. 6—Variation of first order rate constant during reduction of American grade ZnO samples.

graphic samples, some of which are illustrated in Figs. 3 and 4. In general, the photoconductive grade pellets reacted more evenly than the American Grade. The surface roughness of the photoconductive ZnO was also more pronounced at lower temperatures where surface reaction and hence surface heterogeneity is more influential. For the American pellets, both residual porosity and surface heterogeneity are believed responsible for surface roughness, the reaction temperature having little or no effect.

One rule of thumb that pervades the literature on gas-solid reactions states that if the rate shows a strong temperature dependence, surface kinetics are controlling. This particular generalization, however, does not apply to ZnO reduction. As discussed above, the external transport model also shows a strong temperature dependence because of the unusual effect of the equilibrium constant. In general, the rule of thumb about apparent activation energies must be used with caution whenever large heat effects are associated with the reaction. Over certain temperature ranges, endothermic and exothermic reactions limited by diffusion may actually exhibit large positive and negative overall activation energies, respectively. Furthermore, a small positive apparent activation energy for an exothermic reaction does not necessarily imply a diffusion limited process. Instead, it may be an indication of mixed control.

Because the rule of thumb about activation energies does not apply to ZnO reduction, it is difficult to devise a truly critical test for distinguishing between surface reaction and external diffusion control. All data were therefore analyzed in terms of the mixed-regime reduction models described earlier. Because Eqs. [18] and [21] correlated the data equally well,[18] the discussion here is confined to the simplified mixed model. Eq. [21] was solved to compute the point-to-point variation in the first order rate constant, k_r:

$$k_r = R/C[1 - (1 - y_{CO,b})(1 + R/Ck)] \qquad [24]$$

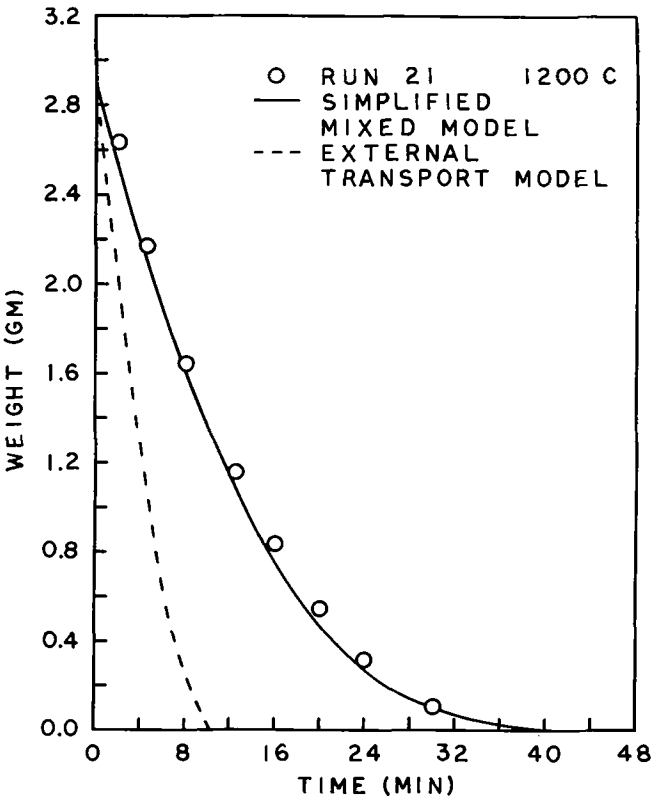

Fig. 7—Arrhenius plot of Eq. [28] for photoconductive grade ZnO.

The particle diameter, mass transfer coefficient, and reduction rate per unit surface were computed assuming a smooth spherical pellet:

$$D = (6w/\pi\rho)^{1/3} \quad [25]$$

$$k = \alpha/D + \beta/D^{1/2} \quad [26]$$

$$R = (dw/dt)/\pi D^2 M \quad [27]$$

Roughness and shape factors could be incorporated into these expressions to account for deviations from the ideal surface, but independent surface and shape measurements would be needed to separate them from the rate constant. In the absence of these measurements, it should be realized that the calculated value of k_r reflects not only chemical kinetics but also deviations from the ideal reacting interface.

Figs. 5 and 6 show typical variations in the rate constant during reduction. Some initial fluctuation occurs, but no long-term trends are apparent. The observed variations during the early stages of reduction probably reflect the initial transition from a sintered smooth surface to a rough reacting interface and the endothermic heat of reaction, which would produce an initial drop in pellet temperature.

Average values for the rate constant were computed for each run, and their logarithms plotted against reciprocal absolute temperature. As shown in Figs. 7 and 8, the first order rate constants exhibit the classical Arrhenius-type temperature dependency. For the photoconductive and American grades, respectively, the following equations yield the best straight lines through the data:

$$k_r = 9.79\,(10^5)\exp\frac{-(37{,}900 \pm 2040)}{\mathcal{R}T} \quad [28]$$

$$k_r = 1.80\,(10^3)\exp\frac{-(20{,}600 \pm 10{,}200)}{\mathcal{R}T} \quad [29]$$

The frequency factors and activation energies were estimated by linear regression, and the error indi-

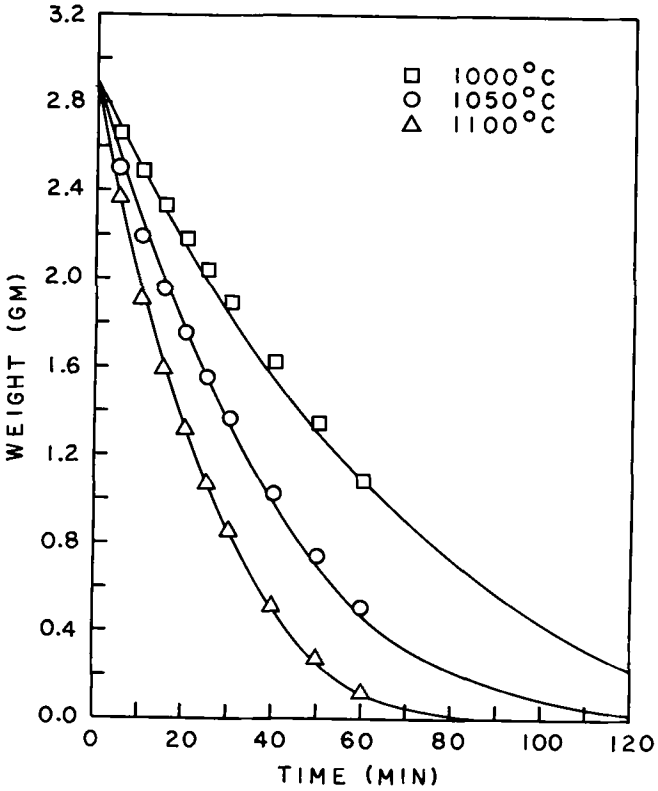

Fig. 8—Arrhenius plot of Eq. [29] for American grade ZnO.

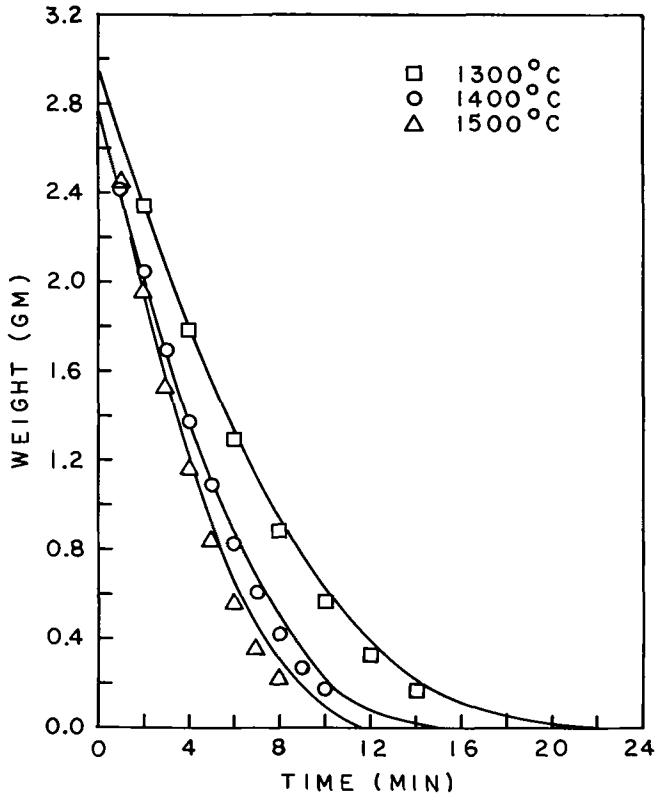

Fig. 9—Comparison of model predictions with data for photoconductive grade ZnO.

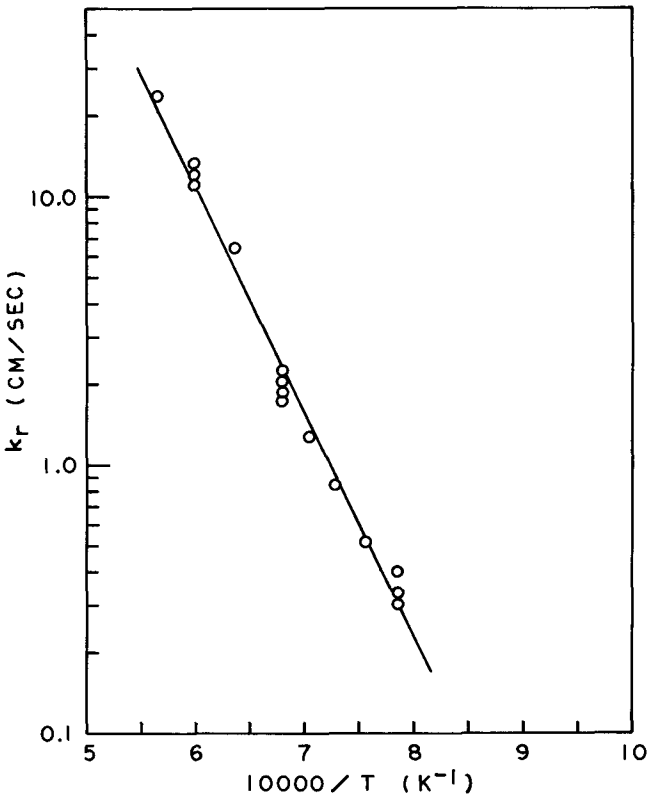

Fig. 10—Comparison of model predictions with data for photoconductive grade ZnO.

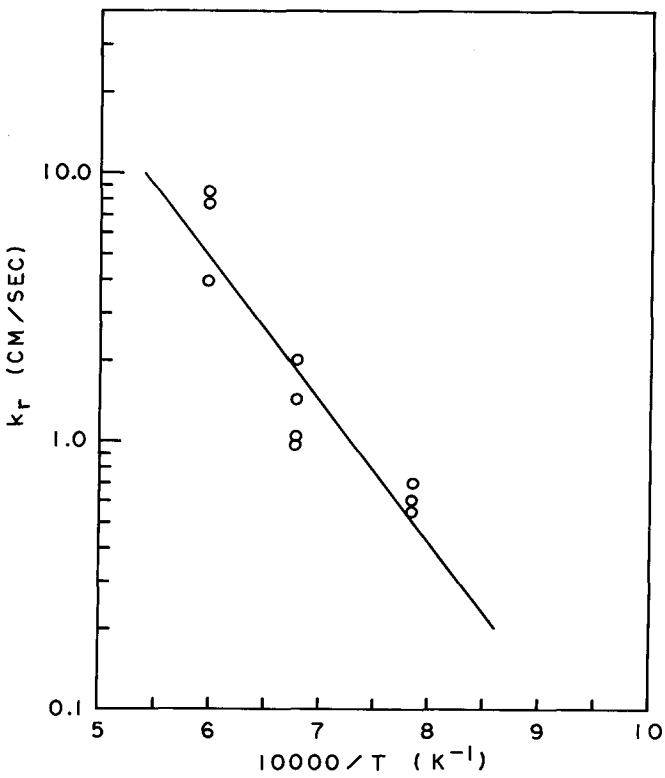

Fig. 11—Comparison of model predictions with data for photoconductive grade ZnO.

cated for each activation energy represents the 95 pct confidence interval. For the American grade oxide, the scatter indicated by the 95 pct confidence limit is considerable.

Fig. 9 shows how well the simplified mixed-regime model fits the weight loss data for the photoconductive grade ZnO at 1200°C. Also presented is the predicted weight loss assuming that external transport (of CO towards and of CO_2 and Zn away from the pellet surface) is completely controlling. Figs. 10 and 11 confirm that the mixed regime model fits the data very well over the entire temperature range from 1000° to 1500°C.

CONCLUSIONS

This work supports the following specific conclusions:

1) Good single particle reproducibility was achieved in reduction of the high purity photoconductive ZnO, but considerable scatter was encountered with the less pure American Grade. Commercial grades may be expected to exhibit even wider variations in reproducibility.

2) Reduction of dense, high purity, photoconductive-grade ZnO pellets with CO can be adequately described by a two-step model which postulates an external diffusion step acting in series with a first order irreversible chemical reaction step at the surface. The chemical reaction step exhibits an activation energy of 37,900 (±2040) cal per mole.

3) Results for the American grade ZnO indicate that impurities, primarily silica and alumina, inhibit the rate at high temperatures.

This study also refutes the "rule of thumb" which states that a strong temperature dependence indicates that surface reaction is controlling. Highly endothermic and exothermic reactions can exhibit large positive and negative apparent activation energies, respectively, even when the overall rate is controlled entirely by diffusion. This occurs over the temperature range where the equilibrium conversion changes rapidly.

NOMENCLATURE

Upper Case

C	total molar gas concentration, mole per cu cm; $C = P/RT$ for an ideal gas mixture.
$C_{i,s}$	molar concentration of component i at the pellet surface, mole per cu cm; i = CO, CO_2, Zn, I (inert).
D_0, D	initial and instantaneous particle diameter, cm.
K	thermodynamic equilibrium constant for the ZnO reduction reaction, atm.
K_c	concentration equilibrium constant for the ZnO reduction reaction, mole per cu cm.
M	molecular weight of ZnO, 81.38 g per mole.
N_i	molar flux of ith component, mole per sq cm per sec.
P	total pressure, atm.
R	reduction rate of ZnO per unit area of surface, mole per sq cm per sec.

S	external pellet surface, sq cm.
T	absolute temperature, °K.
V	free stream or bulk gas velocity, cm per sec.

Lower Case

d	differentiation operator.
k	instantaneous mass transfer coefficient, cm per sec.
k_r	first order specific reaction rate constant, cm per sec.
t	time, sec.
w	instantaneous pellet weight, g.
x	spatial coordinate, cm.
y_i	mole fraction of ith species.
$y_{i,b}$, $y_{i,s}$	mole fraction of ith species in the bulk gas and at the pellet surface, respectively.

Script

$\mathfrak{D}$	common diffusivity for the CO, CO_2, Zn system, sq cm per sec.
$\mathfrak{R}$	universal gas constant, 1.987 cal per mole, °K, or 82.1 cu cm, atm per mole, °K.

Greek

α	dimensional constant defined by Eqs. [15] and [16], sq cm per sec.
β	dimensional group defined by Eqs. [15] and [16], $cm^{3/2}$ per sec.
γ	dimensionless group $\alpha/\beta D_0^{1/2}$.
δ	hypothetical film thickness, cm.
ρ	density of ZnO, 5.6 g per cu cm.
ρ_g	gas density, g per cu cm.
μ	gas viscosity, poise.
ψ	dimensionless group $\alpha/(1 + y_{CO,b})D_0 k_r$

ACKNOWLEDGMENTS

The authors thank the St. Joe Minerals Company for four successive Chemical Engineering Fellowships at Carnegie-Mellon University. In addition the St. Joe Minerals Company very kindly bought the special high-temperature furnace used in this study. Specifically, the authors wish to acknowledge Dr. R. E. Lund and Dr. C. C. Long of the St. Joe Minerals Company, and Dr. R. S. Bowman of Mellon Institute for helpful and interesting discussions on various aspects of this research.

REFERENCES

1. G. Tammann and A. Ya. Zvorukin: *Z. Anorg. Allgem. Chem.*, 1928, vol. 170, pp. 62-70.
2. W. Baukloh and F. Springorum: *Z. Anorg. Allgem. Chem.*, 1937, vol. 230, pp. 315-20.
3. M. Bodenstein: *Trans. Am. Electrochem. Soc.*, 1927, vol. 51, pp. 365-76.
4. P. V. Gel'd, *et. al.: Doklady Akad. Nauk. SSSR*, 1951, vol. 78, pp. 693-96.
5. P. V. Gel'd, *et. al.: Zhur. Priklad. Khim.*, 1952, vol. 25, pp. 121-33.
6. A. D'Hooghe: *Bull. Sci. Acad. Roy. Belg.*, 1923, vol. 9, No. 5, pp. 323-26; *Chem. Zentr.*, 1924, vol. I, pp. 409-10.
7. J. S. Anderson: *Discussions Faraday Soc.*, 1948, No. 4, pp. 163-73.
8. W. A. Oates and D. D. Todd: *J. Australian Inst. Metals*, 1962, vol. 7, pp. 109-14.
9. K. Hauffe: *Informal Proc. Buhl Intern. Conf. Mater., Pittsburgh*, 1963; 1964, pp. 37-51.
10. T. Imoto, *et. al.: Nippon Kagaku Zasshi*, 1964, vol. 85, No. 1, pp. 9-13.
11. T. Imoto, *et. al.: Nippon Kagaku Zasshi*, 1964, vol. 85, No. 12, pp. 843-45.
12. E. C. Truesdale and R. K. Waring: *AIME Trans.*, 1944, vol. 159, p. 97.
13. C. E. Guger: Ph.D. Thesis, Department of Chemical Engineering, Carnegie-Mellon University, Pittsburgh, Pa., pp. 19-39, 1969.
14. H. L. Toor, and K. R. Arnold: *I&EC Fund.*, 1965, vol. 4, p. 363.
15. R. B. Bird, W. E. Stewart, and E. N. Lightfoot: *Transport Phenomena*, pp. 658-66, J. Wiley and Sons, New York, 1960.
16. W. E. Ranz and W. R. Marshall, Jr.: *Chem. Eng. Progr.*, 1952, vol. 48, pp. 141-46, 173-80.
17. N. Scrivner: Ph.D. Thesis, Department of Chemical Engineering, Carnegie-Mellon University, Pittsburgh, Pa.; C. E. Guger, Ph.D. Thesis, pp. 55-57, 1969.
18. C. E. Guger: Ph.D. Thesis, pp. 99-100, 1969.